Eur. Phys. J. B **33**, 347–354 (2003)
DOI: 10.1140/epjb/e2003-00175-6

THE EUROPEAN PHYSICAL JOURNAL B

Universal properties of shortest paths in isotropically correlated random potentials

R. Schorr[a] and H. Rieger

Theoretische Physik, Universität des Saarlandes, Postfach 15 11 50, 66041 Saarbrücken, Germany

Received 20 December 2002 / Received in final form 10 April 2003
Published online 20 June 2003 –

Abstract. We consider the optimal paths in a d-dimensional lattice, where the bonds have *isotropically correlated* random weights. These paths can be interpreted as the ground state configuration of a simplified polymer model in a random potential. We study how the universal scaling exponents, the roughness and the energy fluctuation exponent, depend on the strength of the disorder correlations. Our numerical results using Dijkstra's algorithm to determine the optimal path in directed as well as undirected lattices indicate that the correlations become relevant if they decay with distance slower than $1/r$ in $d = 2$ and 3. We show that the exponent relation $2\,\nu - \omega = 1$ holds at least in $d = 2$ even in case of correlations. Both in two and three dimensions, overhangs turn out to be irrelevant even in the presence of strong disorder correlations.

PACS. 05.40.-a Fluctuation phenomena, random processes, noise, and Brownian motion – 05.50.+q Lattice theory and statistics (Ising, Potts, etc.) – 64.60 Ak Renormalization-group, fractal, and percolation studies of phase transitions – 68.35.Rh Phase transitions and critical phenomena

1 Introduction

Optimal paths have been a subject of intensive studies during the recent years. Besides being one of the simplest problems involving disorder, this interest can be traced back to the relevance of this problem to various fields, such as polymer models [1–3], surface growth [4], random bond ferromagnets [5–7], spin glasses [8], and the traveling salesman problem [9].

The model under consideration is easily sketched: given an arbitrary weighted graph, each edge has a particular cost. The optimal or shortest path connecting two sites is the one of minimal weight, which is the sum of all costs along that path. We do not restrict to a particular geometry yet as well as we do not specify the costs more precisely so far. In the simplest case, we choose them from a set of random numbers that are uniformly distributed. In this context, the *directed* polymer model has drawn the most significant attention during the past years [1,2,10–12], where one assumes in $d = 2$ a simple square lattice being cut along its diagonal and oriented as a triangle with the diagonal as its base. One allows only paths in the direction to the base, *i.e.*, the path cannot turn backwards. The costs of the edges that belong to the shortest path are interpreted as potential energies for a polymer configuration that passes through these edges (or bonds).

We may now ask whether the properties (scaling exponents) of the shortest path are either influenced by the distribution of the random numbers or the geometry of the lattice. The former is still discussed [1,13–16]. As far as the latter is concerned, it seems to be clear that the universal properties are not changed if the randomness is uncorrelated. For this case Schwartz *et al.* [17] investigated directed and undirected paths in $d = 2, 3$ using Dijkstra's algorithm to find the shortest path and Marsili and Zhang [18] used a transfer matrix method approach considering directed and undirected paths up to $d = 6$. Both state that overhangs exist but nevertheless they suggest that both problems belong to the same universality class, even in high dimensions where overhanging configurations are entropically favored. It is not *a priori* clear that this observation remains true for correlated disorder. In fact, as we will point out below, the average number of overhangs increases for strongly correlated disorder indicating that they might become relevant for strong enough correlations.

In the present study, we study the universal properties of shortest paths and focus on the effect of isotropically correlated random weights on the scaling exponents. To this end, we consider directed and undirected lattice-graphs in two and three dimensions with bond weights $\eta_{\mathbf{j}}$, where the d-dimensional index vector $\mathbf{j} = i_1, ..., i_d \in \mathbb{Z}^d$ denotes the position of a particular bond in the lattice. The total energy or cost of a path $\mathcal{P}$ from one end of the lattice (*e.g.* from one special site or node in the top layer)

[a] e-mail: schorr@lusi.uni-sb.de

to the opposite end (*e.g.* to an arbitrary site or node in the bottom layer) is simply the sum of these bond weights

$$E = \sum_{\mathbf{j}\in\mathcal{P}} \eta_{\mathbf{j}} \; . \tag{1}$$

The weights $\eta_{\mathbf{j}}$ are *correlated* positive random variables, which we define below. We choose the index vector $\mathbf{j}$ of the bonds in such a way that it is identical with the position of the center of the bonds in an Euclidean lattice. *E.g.* for the square lattice ($2d$) in which we define the upper left corner as the origin, all indices take on odd values. We refer to isotropic correlations if the connected correlation function of the costs $\eta_{\mathbf{j}}$ decays with a power law with Euclidean distance of two bonds, *viz.*

$$G(\mathbf{j},\mathbf{j}') = \langle \eta_{\mathbf{j}}\eta_{\mathbf{j}'}\rangle - \langle\eta_{\mathbf{j}}\rangle\langle\eta_{\mathbf{j}'}\rangle \sim |\,\mathbf{j}-\mathbf{j}'\,|^{2\rho-1}, \tag{2}$$

where $\rho < 1/2$. Here $\langle\cdots\rangle$ denotes the disorder average, *i.e.* an average of the probability distribution of $\eta_{\mathbf{j}}$.

For $\rho = 0$ model (1) with (2) represents an effective single vortex line model for interacting vortex lines in a random vector potential [19]. We would like to emphasize that *isotropic* correlations have not been investigated so far: For historical reasons one discriminates between $d-1$ transverse or spatial directions and 1 longitudinal or time direction. This can be traced back to the relation between directed polymers and the KPZ-equation. If the randomness is only correlated in $d-1$ dimensions and uncorrelated in the remaining direction one refers to *spatially* correlated randomness, if the correlations are only present in time direction one refers to *temporal* correlations. Let $\mathbf{j} = (\mathbf{x},t) = ((i_1,...,i_{d-1}),t)$. Then we can describe both cases by $G \sim |\,\mathbf{x}-\mathbf{x}'\,|^{2\rho-1}\cdot\delta(t-t')$ (spatial correlations) and $G \sim |\,t-t'\,|^{2\theta-1}\cdot\delta(\mathbf{x}-\mathbf{x}')$ (temporal correlations).

The first systematic numerical work done on spatially correlated noise is due to Amar *et al.* [20]. Their results are in agreement with the dynamical [21] and functional RG [22,23] predictions. Subsequent careful work by Peng *et al.* [24] and Pang *et al.* [25] was done. As far as temporal correlations are concerned, we refer to the simulation of a ballistic deposition model by Lam *et al.* [26].

In this paper we study *isotropically* correlated disorder, it is organized as follows: In Section 2 we introduce the models, the numerical method and the quantities that we are interested in. In Section 3 we present our results and in Section 4 we summarize our findings.

One remark on the notation: We will use the words graph and lattice as well as costs and energy, node and site and edge and bond synonymously throughout the paper.

2 Model

The *undirected graph* can be described as follows (see Fig. 1b): we choose a simple lattice structure and define one longitudinal and $d-1$ transversal directions. We will refer to them by means of t and $\mathbf{x}$ respectively. We assume the lattice to be periodic in space ($\mathbf{x}$) with period H and L to be the longitudinal size. We choose the origin of the coordinate system as being the starting point (the source) of the path. We assign a particular amount of energy to each bond, whereby these energies are isotropically correlated. Generating these random numbers we follow the method introduced by Pang *et al.* [25]. We infer periodicity and symmetry of the correlator g_ρ in any direction, where

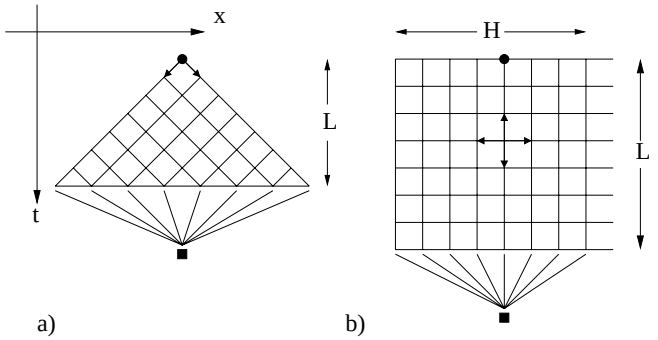

Fig. 1. a) The *directed* graph can be regarded as a square lattice that was cut along its diagonal and oriented as a triangle with the diagonal is its base. The paths are directed downwards to the base. b) In the *undirected* case the path is allowed to turn back on a lattice with periodic boundary conditions in the spatial direction(s). In both cases one fixes the source ●, whereas the target ■ is the most favorable node of the base.

$$g_\rho(\Delta\mathbf{j}) := G(\,\mathbf{j},\mathbf{j}+\Delta\mathbf{j}\,) = |\Delta\mathbf{j}|^{2\rho-1} \tag{3}$$

with $g_\rho(...,(\Delta\mathbf{j})_i + p_i,...) := g_\rho(...,(\Delta\mathbf{j})_i,...)$ and $g_\rho(...,(\Delta\mathbf{j})_i,...) = g_\rho\,(...,p_i/2 - |\,(\Delta\mathbf{j})_i - p_i/2\,|,...)$ in case of a period p_i in direction i. In contrast to pure spatial and temporal correlations where the correlator is taken to be the product of two separate ones, one for the time direction and one for the remaining spatial coordinates, here it is due to a generic vector $\Delta\mathbf{j}$. Adapting the correlator to the lattice, we require a period H in the transversal and $2L$ in the longitudinal direction. By means of the factor 2 we guarantee that $g_\rho(t)$ has the required form (3) in the range $1 \le t \le L$. Its Fourier transform yields $S_\rho(\mathbf{k})$ such that the correlator in the $\mathbf{k}$-space is given by $\langle\eta_{\mathbf{k}}\eta_{\mathbf{k}'}\rangle \sim \delta_{\mathbf{k}+\mathbf{k}',0}\,S_\rho(\mathbf{k})$. Choosing $\eta_{\mathbf{k}} \equiv \sqrt{S_\rho(\mathbf{k})}(r_{\mathbf{k}} - 1/2)\,\exp(2\pi\mathrm{i}\phi_{\mathbf{k}})$, that relation can be fulfilled, where $r_{\mathbf{k}}$ and $\phi_{\mathbf{k}}$ are random variables uniformly distributed between 0 and 1. A transformation back to real space provides the random numbers correlated according to the power law rule (see also Appendix A).

From the set of L^{d-1} optimal paths that connect the source $(\mathbf{x},t) = (\mathbf{0},0)$ with nodes of the bottom layer with coordinates $(\mathbf{x},L)$, we select the shortest one. Technically this is achieved not by repeating the same calculation L^{d-1} times (*i.e.* once for each end-point) but by introducing an extra target node connected to the bottom layer by zero-weight bonds. The algorithm that computes the optimal paths in polynomial time is Dijkstra's algorithm that works in any graph with non-negative weights.

Our study is focused on the universal characteristics of the optimal path, *i.e.* on the scaling exponents ν, the roughness exponent, and ω, the energy fluctuation exponent. ν describes the fluctuations of the path with regard

to a line parallel to the t-axes that is shifted to the origin by an amount matching to the mean position $\langle \mathbf{x} \rangle$ of the polymer. We refer to these fluctuations by D. Due to the direct mapping between the model of shortest paths and growing interfaces [4], it is immediately seen that the energy of the polymer also fluctuates, where we consider several realizations of disorder, we have:

$$D \sim t^{\nu} \qquad \Delta E \sim t^{\omega}. \tag{4}$$

There is no need to modify these relations when we consider *directed paths*. For this purpose we introduce directed bonds, *e.g.*, we restrict to the positive axes. In order to determine the roughness of the polymer, we refer to a line parallel to the bisecting line $(\mathbf{x}, t) \sim (1^{d-1}, 1)$ that crosses the origin. For each size L we can determine the distance of the target node to that line by considering the projection of its position vector onto the bisector. That is, a directed path connects the source $(\mathbf{x}, t) = (\mathbf{0}, 0)$ and the sites on the line between $(0, L)$ and $(L, 0)$, what has to be extended to the notion of a plane in $d = 3$.

As far as undirected paths are concerned one has to make clear how $\mathbf{x}(t)$ can be defined if overhangs appear. In that case $\mathbf{x}(t)$ is not a single valued quantity anymore. We have checked the relevance of several choices but finally we took $\mathbf{x}(t) = \max\{\mathbf{x}_i(t)\}$ with t constant for all $\mathbf{x}_i$. The numerical results that we present are independent of this choice.

As there are $\mathcal{O}(2^n)$ undirected paths across the lattice, where n is the number of nodes, an efficient method is needed that terminates within a reasonable time, such as Dijkstra's algorithm [17,27], that is able to generate the shortest path in polynomial time. In this algorithm the path is successively constructed, *i.e.*, one obtains not only a single path but a cluster of them with energy labels smaller than a certain limit, so that a growth front is established. This cluster contains the so called permanently labeled sites. The algorithm proceeds by extending the front by this site that is the nearest neighbor to it with respect to the energy. If the growth front reaches the base of the lattice we are enabled to reconstruct the shortest path. The growth process of that front can directly be mapped onto a growing Eden cluster [4] providing the same scaling behavior as directed polymers.

If we assume uncorrelated costs the roughness of the growth front scales like the energy fluctuations of the polymer. Since the properties of the surface are described by the KPZ-equation and, consequently, the height-height correlation increases according to a power law with exponent $\omega = 1/3$, we expect in $d = 2$ the scaling exponents of the optimal path of size:

$$\omega_{\mathrm{OP}} = \beta_{\mathrm{KPZ}} = 1/3 \qquad \nu_{\mathrm{OP}} = 1/z_{\mathrm{KPZ}} = 2/3.$$

Exact values are only accessible in $d = 2$. The value of the exponent ν can be extracted from ω if we take into account the exponent relation

$$2\,\nu - \omega = 1$$

which holds for uncorrelated noise. This relation follows from the Galilean invariance of the KPZ-equation and the transfer to shortest paths afterwards. In $d = 3$ there exist no analytical predictions. Nevertheless, the estimates of numerous numerical studies [1,2,17] yield

$$\omega \approx 0.19 \qquad \nu \approx 0.62.$$

As long as the Galilean invariance holds, the scaling relation remains unchanged. This invariance is not altered in the presence of spatial (transversal) correlations but it is broken in the presence of temporal (longitudinal) correlations.

A Flory type argument [11] leads to the following estimate ν_F of the roughness exponent as a function of ρ. A continuum Hamiltonian of the energy (1) has to include an elastic part, since this is generated in a coarse graining procedure.

$$\mathcal{H} = \int \mathrm{d}t \, \left[\frac{\lambda}{2} (\nabla_t \, \mathbf{x})^2 + \eta(\mathbf{x}, t) \right]. \tag{5}$$

Rescaling t with a factor b and x with a factor b^{ν} the elastic term scales with $b^{\,2\nu-2}$ and the disorder term with $b^{\,\rho-1/2}$ (because of the power law decay of the disorder correlations), resulting in

$$\nu_F = \frac{1}{2}\,\rho + \frac{3}{4}. \tag{6}$$

In case of uncorrelated random numbers the disorder term scales with $b^{\,-\nu(d-1)/2-1/2}$, resulting in

$$\nu_{uncorr.} = \frac{3}{d+3}. \tag{7}$$

Hence we expect

$$\nu = \begin{cases} \nu_{uncorr.} & \text{for} \quad \rho \leq \frac{3(1-d)}{2(3+d)} \\ \nu_F & \text{for} \quad \rho > \frac{3(1-d)}{2(3+d)}. \end{cases} \tag{8}$$

This simplified scaling picture should yield at least a lower bound for the roughness exponent.

3 Numerical results

In addition to the relations in (4), we define the two exponents γ and δ by $l \sim L^{\gamma}$ and $B \sim L^{\delta}$, where B is the number of backward bonds with respect to time, and l is the total length of the path. We also determine the fractal dimension d_c of the shortest path cluster $M \sim L^{d_c}$, where M is the mass of its surface. The shortest path cluster consists of all nodes with labels smaller than a maximal one given by the shortest path weight from the source to the base. As far as Dijkstra's algorithm is concerned, its surface is constituted by all the sites that are part of the growth front with at least one nearest neighbor that is not yet permanently labeled.

The scaling exponents are extracted from a set of data that reproduces the simulation of several lattice sizes (Fig. 2). The statistical error is usually smaller than the

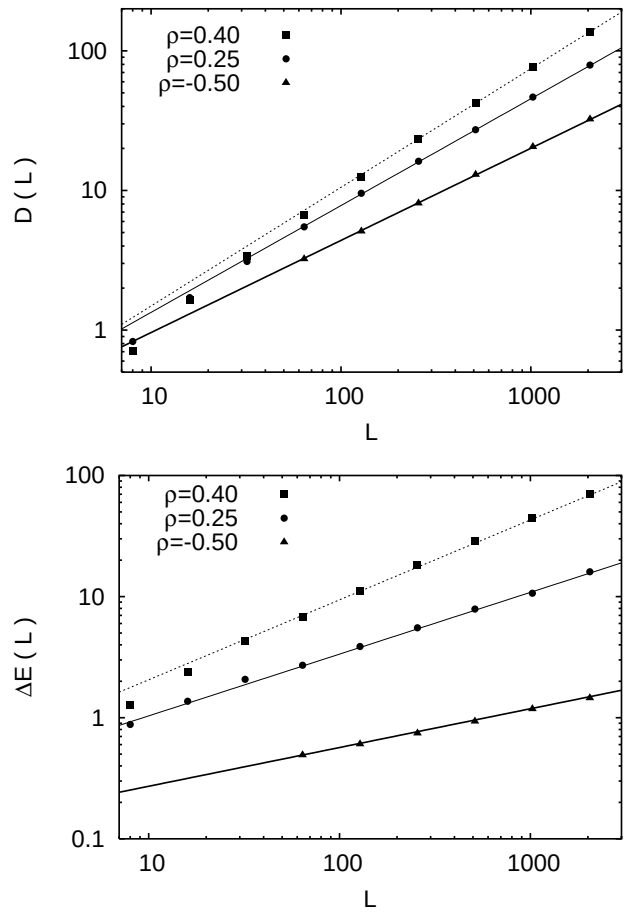

Fig. 2. Scaling of the height-height correlation $D(L)$ and the energy fluctuations $\Delta E(L)$ in $d = 2$ for NDOPs. The straight lines are least square fits of the data for $L > 100$ to a power law $D(L) \propto L^{\nu}$ and $\Delta E(L) \propto L^{\omega}$ with $\nu = 0.66, 0.77, 0.85$ and $\omega = 0.32, 0.50, 0.67$ for $\rho = -0.50, 0.25, 0.40$. The statistical error of the data for $D(L)$ and $\Delta E(L)$, which are averaged over at least 10 000 disorder realizations, is smaller than the symbol size.

symbol size. We adapt the transversal expansion H to the size L in such a way that we eliminate further effects on our data by increasing H, even if $\rho = \rho_{max}$. Finally, we consider lattices of size $H \geq 4L$ if $L \leq 2048$ and $H = 4096$ if $L = 2048$ in $d = 2$, as well as $H = 128$ if $L \leq 32$ and $H = 256$ if $L \geq 64$ in $d = 3$. At any time, we forbid the shortest path cluster spanning the lattice in order to avoid saturation effects. This requirement cannot be satisfied for all $L = 128$ in case of $d = 3$ and ρ close to ρ_{max}.

Our results are averages over more than 10 000 disorder realizations per size L. The generation of correlated random numbers is the most time consuming part. For each sample we have to perform a Fourier transformation of $N = 2^d L H^{d-1}$ numbers twice. On the average approximately 90% of the CPU time is needed for this execution. Some more information about the generation is given in Appendix A.

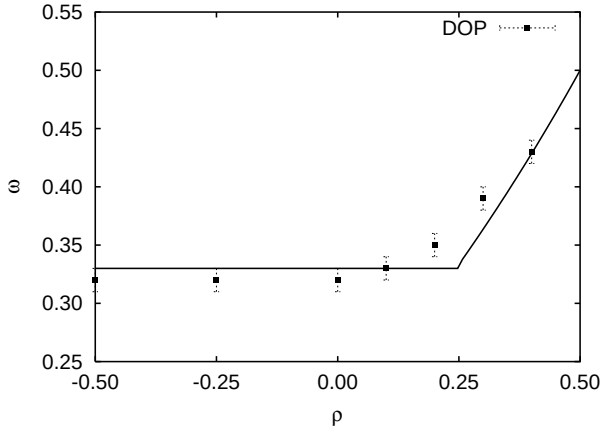

Fig. 3. Our result of the directed path in $d = 2$ for spatial correlations. A direct comparison with the results of [25] (Fig. 3) shows that they are in good agreement. The full line is theoretical prediction from a one-loop KPZ dynamic RG calculation [21] and a DPRM functional RG [23] calculation.

As a first check we studied the directed polymer problem in $d = 2$ with only spatially correlated bond weights as it was done by Pang *et al.* [25]. It can be seen from Figure 3 that we are in very good agreement with their results. In case of strongest correlations ($\rho = 0.40$) we obtain $\nu = 0.71 \pm 0.01$ and $\omega = 0.43 \pm 0.01$. It is quite evident that correlations are only relevant in the regime $\rho > 0$.

Two dimension (d = 2)

In $d = 2$ we find that the roughness exponent ν does not depend on the directedness of the lattice. Overhangs do not play an important role and the undirected path can be regarded as a directed one (Fig. 4). Independent from the strength of the correlations all exponents ν are smaller than the critical value 1. As far as undirected shortest paths are concerned, exceeding that critical value leads to fractal objects that cannot become directed, even on large scales. The errorbars depicted in Figure 4 are not the result of the least square fit but estimates of the minimal and maximal slopes being in nearly perfect agreement with our data.

In contrast, we obtain a less significant data collapse with respect to the energy fluctuation exponent ω, if $\rho > 0$. This may be affected by a statistics that has room of improvement but it indicates a tendency that is especially noticeable in $d = 3$: the stronger the correlation the more significant variations in ω occur. The reason for this relation is not clear to us. In both cases the exponent relation can be satisfied (Fig. 5) where we are in better agreement with $2\,\nu - \omega = 1$ for undirected paths. We learn from Figure 3 that isotropic correlations in the randomness are relevant for $\rho > 0$. The scaling of the energy fluctuations is much more sensitive to passing from white noise to weak correlations ($\rho = -0.5$) in comparison to the roughness. Whereas ν keeps constant ($\nu = 0.66 \pm 0.01$), ω reduces from $\omega = 0.32 \pm 0.01$ to $\omega = 0.29 \pm 0.01$. The number of

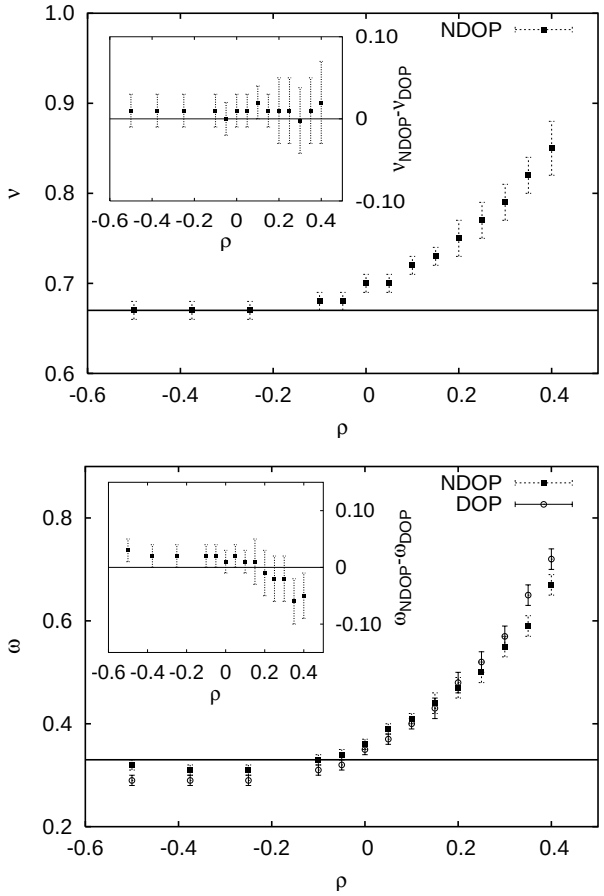

Fig. 4. The scaling exponents ν and ω in $d = 2$ depend on the strength ρ of the correlation. Close to $\rho = 0$ correlations start to affect them significantly. In either case the insets show the difference of both the exponents of the undirected and directed lattice respectively. The reference lines represent the values $\nu = 1/3$ and $\omega = 2/3$ respectively.

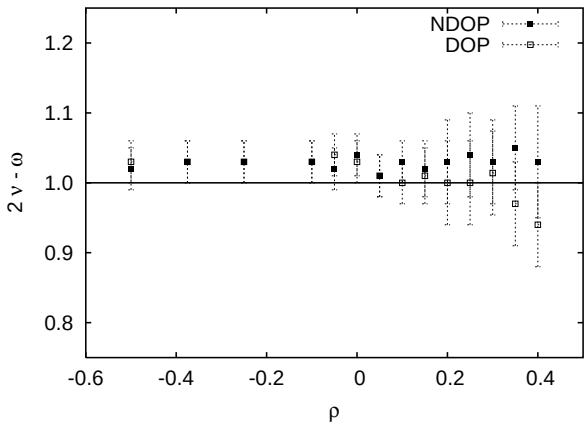

Fig. 5. The exponent relation is depicted for the NDOP model in $d = 2$. Both data sets diverge only close to $\rho = 0.40$ according to the insets of Figure 4.

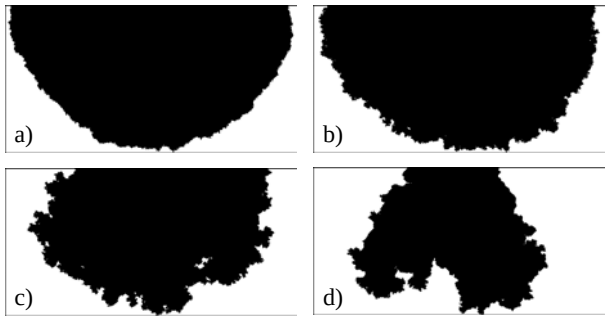

Fig. 6. Realizations of the shortest path cluster (NDOP) for $H = 512$ and $L = 256$. In each case the growth process stops when the growth front reaches the base of the lattice. We choose a) uncorrelated random numbers and correlated random numbers with b) $\rho = 0$, c)+d) $\rho = 0.40$.

backward bonds in the NDOP model remains negligibly small. It is $B \approx 15$ for $L = 1024$ if $\rho = 0.40$ where $\delta \approx 1.0$. In that case almost every path has at least one such bond. According to these results we obtain $l \sim L$.

Although the roughness exponent increases significantly for $\rho \geq 0.3$ and might even come closer to 1 for $\rho \approx 0.6$ it stays still smaller than one. Also the length of the shortest path scales linearly with L for the values of ρ that we could study. Both observations imply a non-fractal shortest path. However, the properties of the shortest path cluster change remarkably when coming closer and closer to $\rho = 0.40$, where the fractal dimension of its surface becomes $d_c \approx 1.1$ instead of $d_c \approx 1$ if $\rho = 0$. In Figure 6 one can see that for weak correlations the surface of the shortest path cluster is a semicircle whereas for larger correlations it becomes topologically more complicated.

Not only the disorder averaged roughness D scales with L^ν but the whole probability distribution $P_L(D)$: It is $P_L(D) = L^\nu p(D/L^\nu)$ as we show in Figure 7 for $\rho = 0.40$. For the scaling function $p(x)$ we can fit a log-normal distribution given by $p(x) = (2\pi\sigma^2)^{-1/2} \exp(-(\ln D/D_0)^2/2\sigma^2)$. The parameters σ and D_0 do not depend on ρ for $\rho \leq 0$ (where $D_0 \approx 0.13$, $\sigma \approx 0.58$) and vary slightly with ρ for $\rho > 0$.

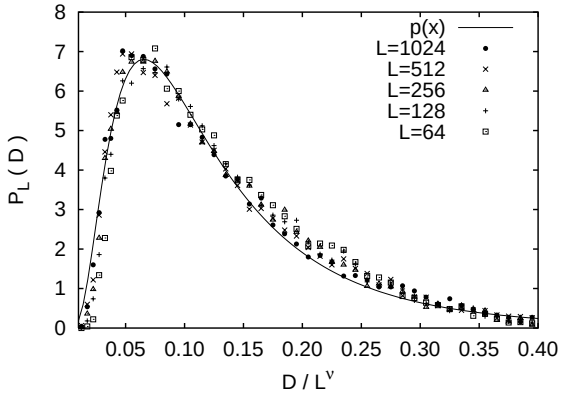

Fig. 7. Scaling plot for the probability distribution $P_L(D)$ of the roughness in case of directed paths for $\rho = 0.40$. The scaling function $p(x)$ is a log-normal distribution with $D_0 = 0.11$ and $\sigma = 0.70$.

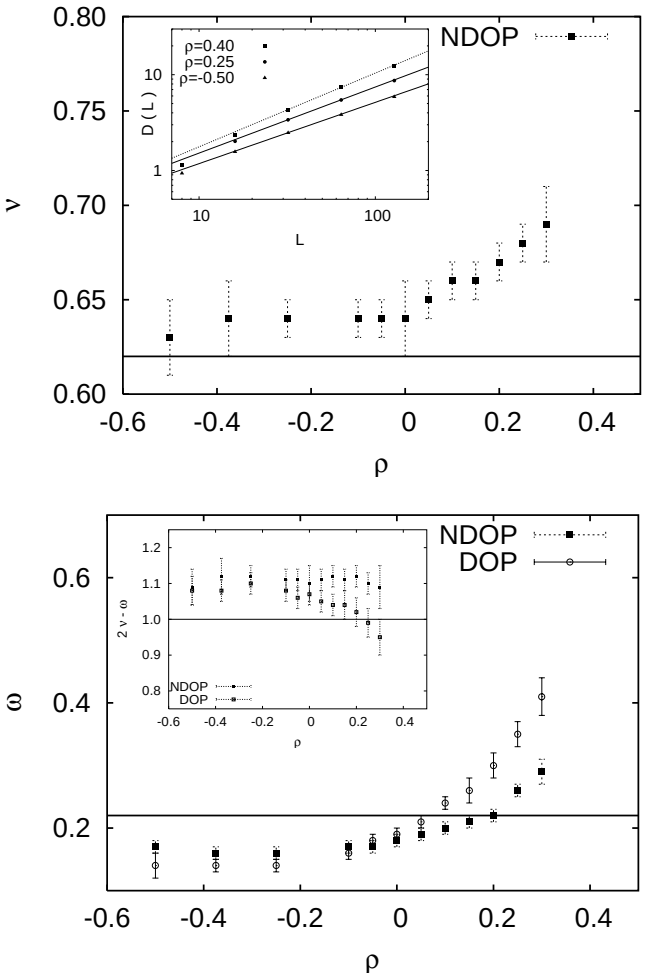

Fig. 8. The exponents ν and ω in $d = 3$ are plotted *versus* ρ. The insets show the scaling of the height-height correlation $D(L)$ for NDOP and the exponent relation in $d = 3$ respectively. The reference lines belong to our results $\nu = 0.62$ and $\omega = 0.22$ in case of uncorrelated numbers.

Three dimensions (d = 3)

The results in $d = 3$ are qualitatively similar to those of the preceding section. For uncorrelated randomness we obtain $\nu = 0.62 \pm 0.02$ and $\omega = 0.22 \pm 0.01$ in agreement with [1,2,17]. Both ν and ω increase monotonously with ρ, *i.e.* increasing correlations. While ν does so without any difference between directed and undirected paths, ω differs from this behavior: the stronger the correlations the more estimates for the exponents deviate from each other (Fig. 8). As $\nu < 1$ the undirected path becomes directed on large scales. We should emphasize that obtaining data in the regime $\rho > 0.25$ for $d = 3$ is much more delicate than in $d = 2$. The local slopes of the energy fluctuations indicate that even for the maximal size $L = 128$ we are not yet in the asymptotic regime for $\rho > 0.3$. Therefore we explicitly restrict ourselves to values $\rho \leq 0.3$. This result refers to both kinds of lattices and, so is not a consequence of saturation effects. The distinct behavior of both kinds

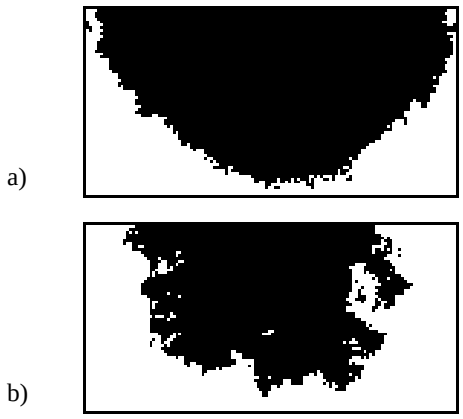

Fig. 9. Cluster of shortest paths in $d = 3$ that is cut along the x-t-plane with $y = H/2$. a) uncorrelated randomness b) strong correlations ($\rho = 0.40$). It is seen that we pass again from a semicircle like cluster to a topologically more complicated one.

of paths can be demonstrated more obviously by plotting the exponent relation $2\nu - \omega = 1$ (see inset of Fig. 8).

Even though the scaling regimes in $d = 3$ are not very wide our estimates for ν and ω deviate significantly from their values in the uncorrelated case. Significantly means here that their estimated errors (obtained in the same way as in our $2d$-study before) are smaller than the deviation from the uncorrelated values. Therefore we can infer that for strong enough correlations ($\rho \geq 0.3$) the DOP and NDOP problems constitute new universality classes. The precise determination of the critical value for ρ, beyond which correlations become relevant, is, however, beyond our numerical precision.

For completeness we mention that even in case of $L = 128$ and $\rho = 0.40$ the number of bonds turning backward is negligibly small: $B \approx 1.6$ compared to $B \approx 3$ in $d = 2$. We do not expect a significant change in B for larger lattices as this quantity scales by an exponent $\delta \approx 1.0$ but the number of paths including such bonds should increase from 60% to 100%.

In contrast to the difficulties above, the fractal dimension d_c of the surface can be extracted quite clearly. It is $d_c \approx 2.35 \pm 0.10$ if we choose $\rho = 0.40$ in contrast to $d_c \to 2.0$ for uncorrelated numbers. We illustrate the change of the cluster by cutting the system along the x-t-plane. Figure 9 shows such cuts for $y = H/2$ where a) denotes random costs and b) corresponds to strongest correlations.

4 Summary

In the present paper we have considered the effect of isotropically correlated bond weights on the scaling behavior of both undirected and directed paths in two and three dimensions. We found that in $d = 2$ the algebraic correlation of the disorder are relevant for a decay slower than $1/r$ (*i.e.* $\rho = 0$) and the roughness exponent ν and the energy fluctuation exponent ω increase monotonously for

$\rho \geq 0$. The Flory estimate (8) for the roughness exponent is fulfilled as a lower bound of our numerical estimates. A precise value for ρ_c, above which correlations modify the universality class, is hard to estimate numerically, but we observe that it is close to and slightly smaller than zero in $d = 2$ and $d = 3$, in agreement with the Flory argument (8).

Moreover, the results in $d = 2$ indicate that the scaling exponents are independent from the directedness even in case of very strong correlations. In contrast to this, in $d = 3$ directed and undirected lattices yield different results for $\rho > \rho_c \approx 0$ indicating that both cases constitute different universality classes. In $2d$ the scaling relation $2\nu - \omega$ appears to remain valid even for stronge correlations (although Galilean invariance is broken), whereas for $d = 3$ we observe in the directed case significant deviations from it (in the undirected case it appears to remain valid).

Finally we could exclude the possibility that optimal paths become fractal for strong disorder correlations as long as they decay algebraically. As a consequence ν stays smaller than one and overhangs turn out to be irrelevant. This behavior changes if we consider the following disorder correlations: $\langle(\eta_{\mathbf{j}} - \eta_{\mathbf{j}+\mathbf{r}})^2\rangle \propto r^{\alpha}$, with $\alpha > 0$, which increase with distance $r = |\mathbf{r}|$. These type of correlators are relevant for an effective model of dislocations in a vortex line lattice [28]. In this case we found that the optimal paths are fractals with a fractal dimension significantly larger than one and depending on the value of α [29].

This work has been supported by the *Deutsche Forschungsgemeinschaft* (DFG).

Appendix A

Here we explain how to initialize the correlation function $g_\rho(\mathbf{j})$ and we show that $N = 2^d L H^{d-1}$ correlated random numbers have to be created for our purposes. We need to generate $2N$ uncorrelated random numbers and have to perform a Fourier transformation twice. If we consider the simple square lattice of nodes with lattice spacing a we can immediately see that we have to distinguish between positions of nodes and positions of bonds. The latter build a simple lattice that is rotated towards the node lattice by $\pi/4$ with a lattice spacing enlarged by a factor $\sqrt{2}$ (Fig. 10). But we have to create correlations according to positions of *bonds*. Let us assume now this lattice to be a two dimensional array. The most comfortable solution of the generation of correlations due to bond positions is to keep the original lattice structure, meaning we switch to a spacing $a/2$ and finally focus on those positions within this array that correspond to bonds in our lattice. Then we define the center of that lattice (array) and initialize each position of the array by $|\mathbf{j}|^{2\rho-1}$, where $-H/2 \leq \mathbf{j}_i < H/2$ or $-L/2 \leq \mathbf{j}_i < L/2$ is the position vector. This array is called the correlator $g_\rho(\mathbf{j})$. There are two problems: by doing so, we generate twice the quantum of correlated random numbers we really need (the information of the black squared positions) and we still have to discuss how to define $g_\rho(0)$. As mentioned in Section 2, we already have to take into account a factor 2 from the longitudinal expansion so that N becomes $N = 2 \times 2^d L H^{d-1}$, where again all sites in the left part of Figure 10 would be occupied. In order to restrict memory usage we compress the lattice along one axes (here the x-axes), whereby we loose the information of all the positions indicated by open symbols. By doing so, we avoid the necessity of defining $g_\rho(0)$ corresponding to a virtual node at the origin and, consequently, being not part of the right side of Figure 10. More important, N is reduced by a factor 2. Note that the Fourier transform on the compressed lattice also yields the desired correlations.

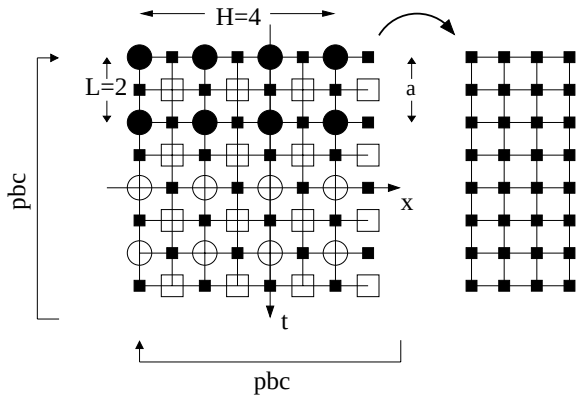

Fig. 10. First we stretch the lattice of size $(H \times 2L)$ resulting in $(2H \times 4L)$ and finally compress it again. Here ● denotes sites that refer to nodes on a lattice of size L and H, ○ corresponds to virtual nodes which have to be introduced in order to follow the definition of the correlator (periodicity in each direction) and ■ refers to bonds. Squares denote positions that additionally arise by switching to a lattice spacing $a/2$. In contrast to black squares the entries of white squares do not play any role concerning the generation of correlated random numbers.

References

1. E. Perlsman, S. Havlin, Phys. Rev. E **63**, 010102 (2001)
2. J.M. Kim, M. A. Moore, A.J. Bray, Phys. Rev. A **44**, 2345 (1991)
3. M. Kardar, Y.-C. Zhang, Phys. Rev. Lett. **58**, 2087 (1987).
4. S. Roux, A. Hansen, E.L. Hinrichsen, J. Phys. A **24**, L295 (1991)
5. D.A. Huse, C.L. Henley, Phys. Rev. Lett. **54**, 2708 (1985)
6. M. Kardar, Phys. Rev. Lett. **55**, 2923 (1985)
7. D.A. Huse, C.L. Henley, D.S. Fisher, Phys. Rev. Lett. **55**, 2924 (1985)
8. M. Mezard, G. Parisi, N. Sourlas, G. Toulouse, M. Virasoro, Phys. Rev. Lett. **52**, 1156 (1984)
9. S. Kirkpatrick, G. Toulouse, J. Phys. Lett. France **46**, 1277 (1985)
10. E. Perlsman, M Schwartz, Europhys. Lett. **17**, 11 (1992)
11. A.-L. Barabási, H.E. Stanley, *Fractal Concepts in Surface Growth* (Cambridge University Press, Cambridge, 1995)

12. T. Vicsek, F. Family, *Dynamics of Fractal Surfaces* (World Scientific, Singapore, 1991)
13. T.J. Newman, M.R. Swift, Phys. Rev. Lett. **79**, 2261 (1997)
14. T. Halpin-Healy, Phys. Rev. E **58**, R4096 (1998)
15. H. Chate, Q.-H. Chen, L.-H. Tang, Phys. Rev. Lett. **81**, 5471 (1998)
16. P. De Los Rios, Phys. Rev. Lett. **82**, 4236 (1999)
17. N. Schwartz, A.L. Nazaryev, S. Havlin, Phys. Rev. E **58**, 7642 (1998)
18. M. Marsili, Y.-C. Zhang, Phys. Rev. E **46**, 4814 (1998)
19. M.S. Li, T. Nattermann, H. Rieger, M. Schwartz, Phys. Rev. B **54**, 16024 (1996)
20. J. Amar, P.-M. Lam, F. Family, Phys. Rev. A **43**, 4548RC (1991)
21. E. Medina, T. Hwa, M. Kardar, Y.-C. Zhang, Phys. Rev. A **39**, 3053 (1989)
22. T. Halpin-Healy, Phys. Rev. Lett. **62**, 445 (1989)
23. T. Halpin-Healy, Phys. Rev. A **42**, 711 (1990)
24. C.-K. Peng, S. Havlin, M. Schwartz, H.E. Stanley, Phys. Rev. A **44**, 2239 (1991)
25. N.-N. Pang, Y.-K. Yu, T. Halpin-Healy, Phys. Rev. E **52**, 3224 (1995)
26. C.-H. Lam, L.M. Sander, D.E. Wolf, Phys. Rev. A **46**, 6128 (1992)
27. A.K. Hartmann, H. Rieger, *Optimization algorithms in Physics* (Wiley VCH, Berlin, 2002)
28. J. Kierfeld, V. Vinokur, Phys. Rev. B **61**, R14928 (2000)
29. R. Schorr, H. Rieger, unpublished